European Journal of Echocardiography (2011) **12**, 19–25
doi:10.1093/ejechocard/jeq092

Dynamic change of mitral apparatus as potential cause of left ventricular outflow tract obstruction in hypertrophic cardiomyopathy

Hye Jin Hwang[1], Eui-Young Choi[1]*, Jun Kwan[2], Sung Ai Kim[1], Chi Young Shim[1], Jong-Won Ha[1], Se-Joong Rim[1], Namsik Chung[1], and Sung Soon Kim[1]

[1]Cardiology Division, Yonsei Cardiovascular Center and Cardiovascular Research Institute, Yonsei University College of Medicine, 134 Shinchon-dong, Seodaemun-gu, Seoul 120-752, South Korea; and [2]Cardiology Division, Inha University College of Medicine, Incheon, South Korea

Received 7 May 2010; revised 9 July 2010; accepted after revision 10 July 2010; online publish-ahead-of-print 7 August 2010

Aims The geometry of the mitral apparatus changes dynamically throughout systole and diastole. We investigated how geometric dynamics of the mitral apparatus could affect the haemodynamics of the outflow tract in patients with hypertrophic cardiomyopathy presenting with systolic anterior motion (HCM_{SAM}) using three-dimensional (3D) echocardiography.

Methods and results We obtained transthoracic volumetric images in 21 patients with HCM_{SAM} with differing trans-left ventricular (LV) outflow tract pressure gradient (PG_{LVOT}) and in 23 controls. Original software was used to crop the 3D data into 18 radial planes; the mitral annulus, leaflets, coaptation point, protruding septum, and papillary muscles (PMs) tips were traced in each plane. The data were then reconstructed for 3D distance measurements and volumetric assessment. Shorter coaptation-septal distance (12 ± 4 vs. 21 ± 3 mm, $P < 0.001$), shorter inter-PM distance (13 ± 5 vs. 18 ± 4 mm, $P = 0.02$), and larger mitral tenting volume/body surface area (TVindex) (2.1 ± 1 vs. 0.5 ± 0.3 mL/m^2, $P < 0.001$) were associated with HCM_{SAM} vs. control. PG_{LVOT} increased with TVindex ($r = 0.51$, $P = 0.01$), and decreased with coaptation-septal distance($r = -0.83$, $P < 0.001$) and the inter-PM distance ($r = -0.69$, $P < 0.001$) at mid-systole but not at mid-diastole (all $P > 0.05$). In addition, the coaptation-septal distance, TVindex, and inter-PM distance correlated each other (all $P < 0.05$). After adjustment for measures of mitral geometric change, the coaptation-septal distance was closely associated with PG_{LVOT} ($\beta = -0.73$, $P < 0.001$).

Conclusion These findings suggest that dynamic geometric changes by interaction of PMs, mitral tenting, and the coaptation point at mid-systole may be important contributors to outflow obstruction in HCM_{SAM}.

Keywords Hypertrophic cardiomyopathy • Left ventricular outflow tract obstruction • Echocardiography

Background

Obstruction of the left ventricular (LV) outflow is an important pathophysiological component of hypertrophic cardiomyopathy (HCM) and is associated with adverse clinical outcomes, such as heart failure and cardiovascular accidents.[1,2] Systolic anterior motion (SAM) of the mitral valve is the cause of dynamic outflow obstruction in most patients with HCM. SAM is caused by the protrusion of the mitral valve leaflet, normally supported by many surrounding structures.[3] Many studies support the concept that primary structural deformities of the mitral apparatus, which includes leaflet elongation (including increased size of both anterior and posterior leaflets or asymmetrical enlargement of either the anterior leaflet or a posterior leaflet scallop), papillary muscle (PM) displacement, abnormal coaptation, and chordal slack[4–11] could be primary causes of SAM. However, it has not yet been determined how these deformities cause haemodynamic changes in the LV outflow tract (LVOT). Structural deformities could be related to LVOT pressure development; however, it is not known how structural deformities

* Corresponding author. Tel: +82 2 2228 8460, fax: +82 2 2227 7943, Email: choi0928@yuhs.ac

primarily observed at the time of diastole in most studies could cause abnormal haemodynamic changes during systole. It is also unknown whether many individual structures or one specific structural deformity affects the pressure gradient in the LVOT. Because the morphology and location of structural deformities can change dynamically throughout systole and diastole, dynamically changed positions of the mitral apparatus in systole could play an important role in creating a haemodynamic obstacle in the outflow tract. We hypothesized that abnormal geometric dynamics of the mitral apparatus in patients with HCM presenting with SAM (HCM_{SAM}) would contribute to haemodynamic disturbance in the outflow tract. Prior experimental studies[7,10] found that the PM tips displaced towards one another to produce relative chordal slack in the central leaflet portions, possibly creating SAM without septal hypertrophy. Accordingly, we sought to investigate whether spatiotemporal changes of the PM and/or mitral tenting, affected by altered PM geometry, would be related to haemodynamic changes in the outflow tract of patients with HCM_{SAM}, using real-time three-dimensional (3D) echocardiography.

Methods

Study population

Forty-one patients were referred for HCM_{SAM} from May 2006 to September 2007. HCM was diagnosed according to criteria of maximal septal thickness $\geq$15 mm and septal to posterior wall ratio $>$1.3 at diastole. Inclusion criteria were: (i) a structurally normal mitral valve, (ii) technically adequate real-time 3D echocardiographic imaging of the LV chamber and the mitral apparatus to allow for analysis of 3D geometry, and (iii) a normal sinus rhythm. Exclusion criteria were: (i) structural valvular or subvalvular lesions (such as mitral valve prolapse or rheumatic disease), (ii) a history of septal reduction by operation or alcohol ablation, and (iii) other cardiac diseases, such as ischaemic cardiomyopathy, pericardial, congenital, or infiltrative heart disease. Four patients had a technically inadequate image, two had a mid-ventricular obstruction, two had aortic stenosis by degenerative change, two had mitral prolapse, three had a history of septal reduction, ten had atrial fibrillation, and seven refused the study. Twenty-one HCM_{SAM} patients were enrolled in the study. Twenty-three control subjects were selected. All patients gave informed consent.

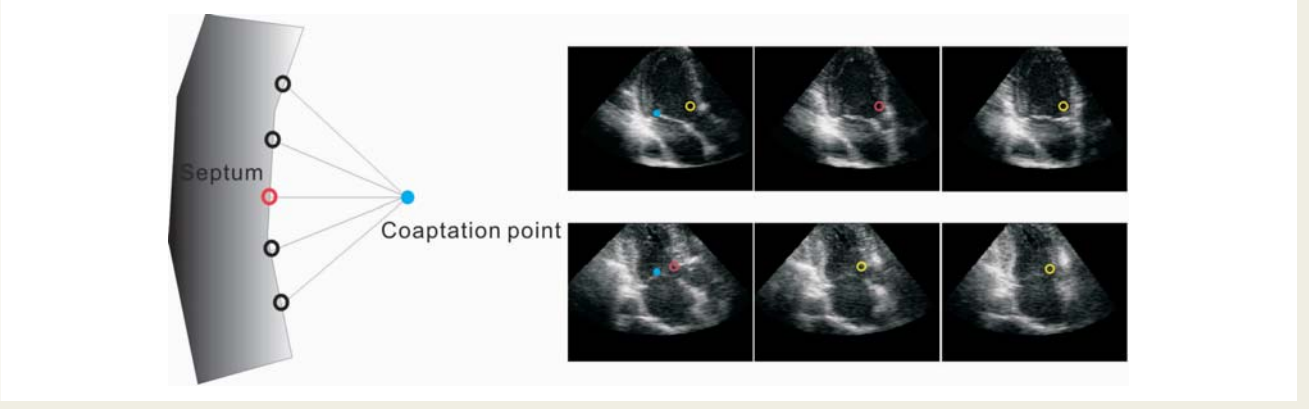

Figure 1 We defined mitral coaptation presented in the 0 view (left plane) as passing through the centre of the aortic valve as a mitral coaptation point (blue circle). To determine the shortest distance from the coaptation point to the septum, a protruding septal point (red or yellow circle) was marked in each plane in control (upper) and obstructive hypertrophic cardiomyopathy (lower) subjects. A red circle indicates the septal point with the shortest distance to the coaptation point as calculated by computer software.

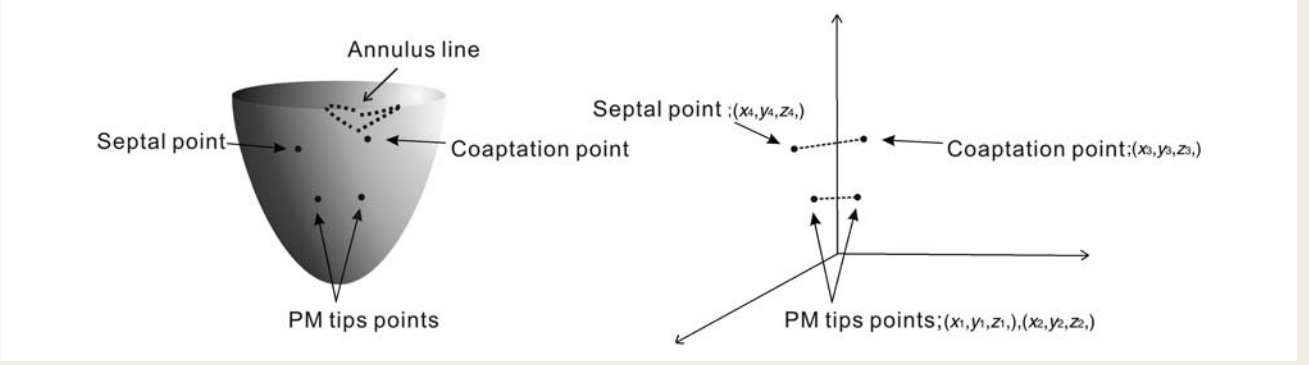

Figure 2 Anatomical points are presented as *x*, *y*, *z* coordinates for three-dimensional distance measurements; the distances between specific points were calculated mathematically by computer software.

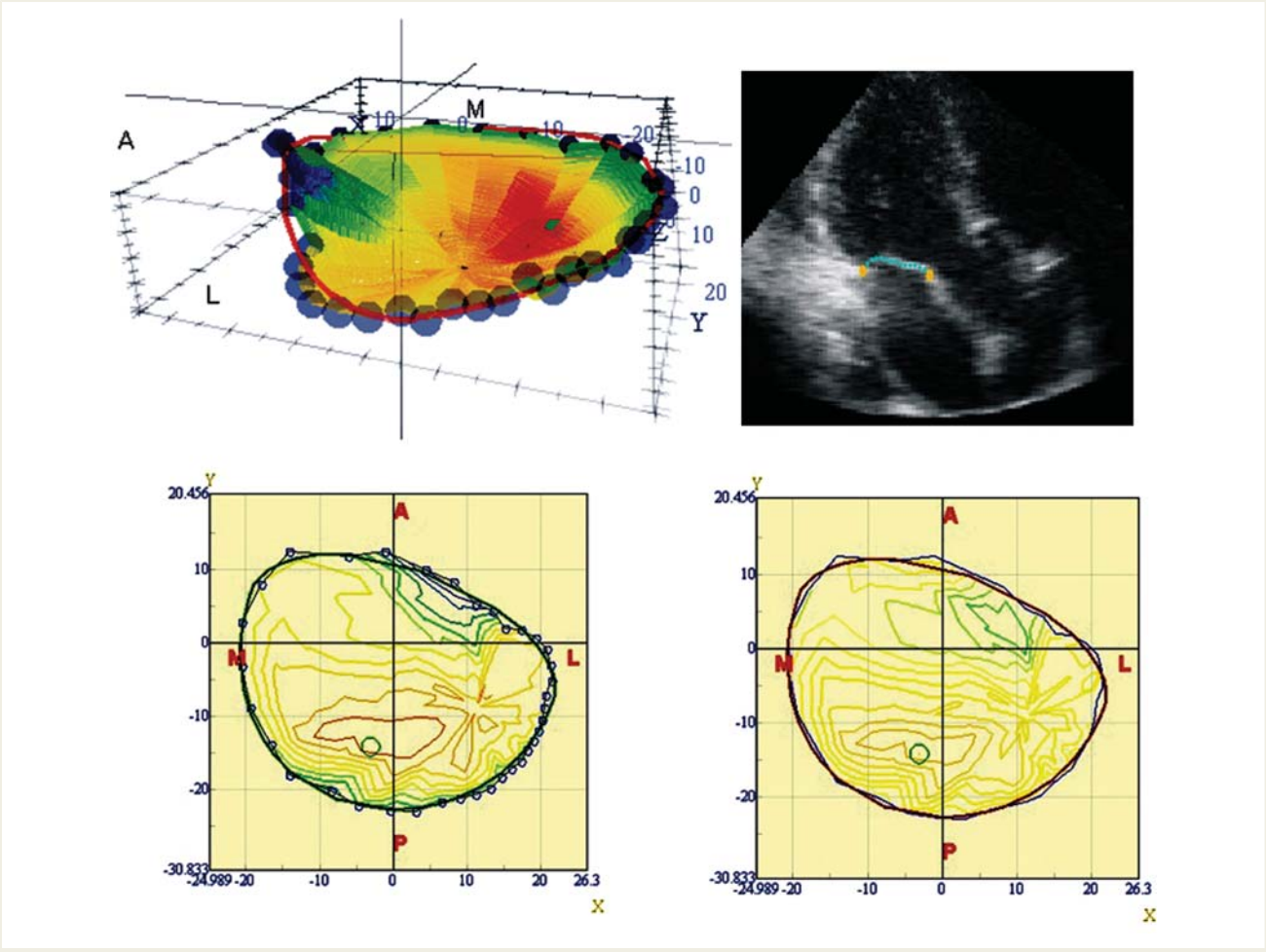

Figure 3 For the three-dimensional quantification of mitral tenting, the actual three-dimensional tenting image (left upper and left lower) was converted to the corrected three-dimensional tenting image (right lower), where the curved mitral annulus was stretched on a flat plane, keeping the distance from the leaflet to the surface of the annulus the same. In the corrected three-dimensional tenting image, maximum tenting length, mean tenting length, and tenting volume were calculated.

Echocardiographic protocol

All echocardiographic exams were performed with a SONOS 7500 (Philips Ultrasound, Bothell, WA, USA) with an S3 probe for 2D imaging and an X4 probe for real-time 3D imaging. All the images were acquired from the left lateral decubitus or the supine position.

Two-dimensional echocardiographic study

All subjects underwent a standard 2D echocardiographic examination. LV posterior wall and septal thickness were obtained with M-mode quantification.[12] The LV diastolic volumes, systolic volumes, and ejection fraction were measured by biplane Simpson's methods and the left atrial volume index was measured by the prolate ellipsoidal method.[12] Continuous-wave Doppler was used to measure maximal velocity across the LVOT and the pressure gradient was estimated by using the simplified Bernoulli equation.[13] The severity of mitral regurgitation was evaluated by vena contracta width of the maximal SAM induced regurgitant colour Doppler jet.[14]

Three-dimensional echocardiographic study

Transthoracic volumetric images (full volume mode) were obtained from the apical view in all subjects. The volumetric frame rate was 16–20 frames/s. All volumetric images were digitally stored and transferred into a personal computer for off-line analysis. We analysed the volumetric images using 3D computer software (YD, LTD, Japan).[15] First, the axis through the apex and the centre of the annulus was set by manually rotating the image, defined to the '*Z*' axis. The volumetric images were automatically cropped into 18 radial planes spaced 10° apart; the 0 view passed through the centre of the aortic valve, where the axis intersecting the *Z*-axis was defined as the '*X*' axis. Tracing was simplified in each cropped plane at mid-systole [peak T on electrocardiogram (ECG)], approximating the time of maximal LVOT velocity. To identify the interaction between structures surrounding the LVOT the annular points, leaflets, tips of the anterolateral PM and posteromedial PM, coaptation points of the MV, and the most protruding septal point were manually traced with different colours in cropped planes. We defined the mitral coaptation presented in the 0 degree view passing through the centre of the aortic valve as a mitral coaptation point (*Figure 1*). All individual anatomical points were presented as '*x*, *y*, *z*' for quantitative measurement; anatomical 3D images of the mitral leaflets and annulus were reconstructed from these data and the distances between specific points were calculated mathematically by computer software (*Figure 2*).

To find out the shortest distance from a coaptation point to the septum, protruding septal points were marked in each plane and the distances between two points of the coaptation point and the septum were calculated mathematically by computer software (*Figure 1*). The shortest distance was defined as the coaptation-septal distance. The tips of two PMs were marked at mid-systole and mid-diastole and the distance between these two points was calculated by software. When the PM tips were not visible or difficult to measure, we moved the axis to accurately identify the PM tips. For the 3D quantification of mitral tenting, the actual 3D tenting image was converted to the corrected 3D tenting image, in which the curved mitral annulus was stretched on a flat plane, keeping the distance from the leaflet to the surface of the annulus the same. In the corrected 3D tenting images, the maximum tenting length, mean tenting length, and tenting volume were calculated (*Figure 3*).

Statistical analysis

Continuous variables are presented as the mean ± SD. Group comparisons used Student's *t*-test for parametric analysis and the Mann–Whitney *U* test for non-parametric analysis. A value of $P < 0.05$ was considered significant. Mutual associations between individual components of coaptation point-septum, mitral tenting, and PM were assessed by Pearson's correlation coefficient. Stepwise multiple linear regression analysis was performed to assess the determinants of the pressure gradient. The univariate correlation coefficients for these variables were determined and entered into a multivariate model for predicting the pressure gradient by use of the SPSS 15.0 statistical package (SPSS Inc., Chicago, IL, USA).

Results

Baseline characteristics

Baseline characteristics of normal subjects and patients with HCM_{SAM} are detailed in *Table 1*. Compared with normal controls, the interventricular septal thickness, left atrial volume index, and ejection fraction were significantly higher in patients with HCM_{SAM} (*Table 1*). The LV end-diastolic volume and end-systolic volume were smaller in the HCM_{SAM} group than in normal controls. The maximal pressure gradient of the LVOT was 48 ± 32 mmHg (range: 4–118 mmHg) and the mean pressure gradient was 22 ± 16 mmHg (range: 3–57 mmHg). The mean vena contract a width of mitral regurgitation was 2.3 ± 3.1 mm (*Table 1*).

Geometry of the mitral apparatus in normal subjects and HCM_{SAM}

Geometric measurements of mitral tenting, PM, and the coaptation point at mid-systole for the two groups are summarized in *Table 2*. The coaptation point was closer to the protruding septum in patients with HCM_{SAM} compared with normal subjects (*Figure 1*). Maximum and mean tenting length and tenting volume/body surface area (TVindex), in corrected 3D tenting images, were significantly higher in patients with HCM_{SAM} compared with normal subjects. The inter-PM distance was shorter in those with HCM_{SAM} than in normal subjects at mid-systole, approximating the time of maximal velocity in the outflow tract (13 ± 5 vs. 18 ± 4 mm, $P = 0.001$), but there was no significant difference between the two groups at mid-diastole (21 ± 3 vs. 22 ± 4 mm, $P = 0.42$).

Table 1 Baseline characteristics and two-dimensional echocardiographic parameters

	Controls ($n = 23$)	HCM_{SAM} ($n = 21$)	*P*
Age, year	48 ± 13	52 ± 11	0.36
Female, *n* (%)	7 (30)	4 (19)	0.38
SBP, mmHg	126 ± 13	117 ± 16	0.16
DBP, mmHg	67 ± 9	70 ± 8	0.12
HR, beats per minute	66 ± 3	63 ± 7	0.22
β-blocker use, *n* (%)	0	13 (62)	
Calcium channel blocker use, *n* (%)	0	10 (48)	
ACE inhibitor or AT blocker use, *n* (%)	0	4 (9)	
LVEDV, mL	113 ± 16	86 ± 21	0.03
LVESV, mL	42 ± 7	22 ± 9	<0.001
LVEF, %	62 ± 8	71 ± 11	<0.001
IVSd, mm	8 ± 1	19 ± 3	<0.001
IVSs, mm	12 ± 1	22 ± 3	<0.001
PWd, mm	9 ± 1	11 ± 3	0.003
LA volume index, mL/m^2	20 ± 4	37 ± 12	<0.001
peak PG_{LVOT}, mmHg		48 ± 32 (4–118)	
mean PG_{LVOT}, mmHg		22 ± 16 (3–57)	
MR vena contracta width, mm		2.3 ± 3.1	

HCM_{SAM} indicates hypertrophic cardiomyopathy and systolic anterior motion of mitral valve leaflets; SBP, systolic blood pressure; DBP, diastolic blood pressure; HR, heart rate; ACE, angiotensin-converting enzyme; AT, angiotensin; LVEDV, left ventricular end-diastolic volume; LVESD, left ventricular end-systolic volume; LVEF, left ventricular ejection fraction; IVSd, interventricular septum thickness at end-diastole; IVSs, interventricular septum thickness at end-systole; PWd, posterior wall thickness at end-diastole; PGLVOT, pressure gradient of the left ventricular outflow tract; MR, mitral regurgitation.

Table 2 Geometric measurements of mitral apparatus

	Controls ($n = 23$)	HCM_{SAM} ($n = 21$)	*P*
Mitral coaptation			
Coaptation-septal distance, mm	21 ± 3	12 ± 4	<0.001
Mitral tenting			
Maximum tenting length, mm	5.9 ± 1.5	8.9 ± 2.7	<0.001
Mean tenting length, mm	2.1 ± 0.9	3.4 ± 1.6	0.002
Tenting volume/BSA, mL/m^2	0.5 ± 0.3	2.1 ± 1.0	<0.001
Papillary muscles (at mid-systole)			
Inter-PM distance, mm	18 ± 4	13 ± 5	0.001

BSA indicates body surface area; inter-PM distance, the distance from the tip of the posteromedial papillary muscle to the tip of the anter-lateral papillary muscle.

Geometric interaction of mitral apparatus for left ventricular outflow tract pressure gradient in systole

The relationships between geometry of the mitral coaptation point, mitral tenting, and PM for LV outflow tract pressure gradient (PG_{LVOT}) at mid-systole are summarized in the *Table 3*. A close inverse correlation between PG_{LVOT} and the coaptation-septal distance ($r = -0.83$, $P < 0.001$), and inter-PM distance ($r = -0.69$, $P < 0.001$) was found. PG_{LVOT} increased in association with the mean tenting length ($r = 0.45$, $P = 0.03$) and calculated TVindex ($r = 0.51$, $P = 0.01$). Coaptation-septal distance decreased with the mean tenting length ($r = -0.48$, $P = 0.02$) and TVindex ($r = -0.47$, $P = 0.02$), and increased with the inter-PM distance ($r = 0.68$, $P < 0.001$). TVindex correlated inversely with the inter-PM distance ($r = -0.47$, $P = 0.02$). PG_{LVOT} also increased with the MR vena contracta width ($r = 0.52$, $P = 0.03$). However, PG_{LVOT} was not correlated with septal thickness, LV systolic and diastolic volumes, LA volume index, or maximum tenting length ($P > 0.05$ in these variables).

The relationship of left ventricular outflow tract pressure gradient to papillary muscle geometry in diastole

PG_{LVOT} was not related to the inter-PM distance as measured at mid-diastole ($P > 0.05$). There was no significant correlation between the inter-PM distance at mid-diastole and the coaptation-septal distance, maximum tenting length, mean tenting length, and calculated TVindex (all *P*-values of >0.05).

Independent predictor for left ventricular outflow tract pressure gradient

In a multiple stepwise linear regression model that evaluated age, sex, heart rate, septal thickness, LV systolic volume and diastolic volume, MR vena contracta width, coaptation-septal distance, TVindex, and inter-PM distance, only the coaptation-septal distance ($\beta = -0.73$, $P < 0.001$) was a significant predictor of PG_{LVOT}.

Discussion

The principal finding of this study was that the mitral coaptation point, mitral tenting, and PMs contributed to the development of PG in the outflow tract by interacting with each other. Many investigators have focused mainly on haemodynamic forces, such as the Venturi effect or flow drag, as causes of dynamic LV outflow obstruction.[3,16] However, some have mentioned the possible effects of underlying morphological or structural abnormalities such as septal hypertrophy,[17,18] displaced PM,[7,11,19] and an elongated residual mitral leaflet.[4,5] We investigated the impact of geometric dynamics of the mitral apparatus, including mitral tenting, coaptation point, and PM that create an altered distribution of tension to the mitral leaflets, as they relate to haemodynamic changes and outflow obstruction. This study found that the location of mitral coaptation towards a protruding septum is strongly associated with the outflow pressure gradient and is related to positional change of PM in systole but not in diastole. The TVindex depends on the distance of two PMs in systole and that the tenting itself had a sequentially weak effect on the PG_{LVOT}. This suggests that movement of the coaptation point towards the outflow tract and tethered leaflets produced by the close proximity of both PM participate in provoking obstruction of outflow by propelling the residual leaflet into the outflow tract stream. The movement and geometric change of the PM occurring in systole may play a key role in determining the outflow pressure gradient, even though the coaptation-septal distance is a statistically independent predictor of PG_{LVOT}.

Integration with previous data

These results support the findings of previous reports, which emphasize the importance of geometric change of the mitral apparatus, such as chordal slack[10,11] and PM displacement, as a mechanism of SAM.[7,11,19,20] Abnormal mitral leaflet coaptation contributes to dynamic LV outflow pressure gradients in HCM.[9,11] Patients with obstructive HCM also have primary displacement of the PM anteriorly and towards one another with a concomitant anterior shift of the mitral valve.[7,19,21] Inward displacement of the PM towards one another, as our results and the previous data suggest, would allow the central leaflet portions to slacken and therefore lead to

Table 3 Correlations between geometric parameters of the mitral apparatus and the pressure gradient of the outflow tract

	Mitral coaptation	Mitral tenting			Papillary muscles
	Coaptation-septal distance	Maximum tenting length	Mean tenting length	Tenting volume/BSA	Inter-PM distance
Peak PGLVOT	−0.83 (<0.001)*	0.32 (0.15)	0.45 (0.03)	0.51 (0.01)	−0.69 (<0.001)
Coaptation-septal distance		−0.41(0.06)	−0.48 (0.02)	−0.47 (0.02)	0.68 (<0.001)
Maximum tenting length					−0.38 (0.08)
Mean tenting length					−0.43 (0.04)
Tenting volume/BSA					−0.47 (0.02)

*All the values are presented as correlation coefficient (*P*-value). Abbreviations as in *Tables 1 and 2*.

SAM. Our results also support the previous study done by Sherrid *et al.*[16] which shows that geometric changes of the mitral apparatus, at the time of SAM occurring, are important determinants of SAM but not Venturi effects. Although past studies examined the individual components of the structurally abnormal mitral apparatus and their relationship with SAM in an anatomical view, they did not demonstrate that the severity of the outflow tract obstruction could be affected by interactive geometric transitions of the mitral apparatus at the time of maximal LVOT velocity. In contrast our study showed that sequential geometric alterations of the mitral apparatus have an impact on the degree of the outflow tract obstruction as well.

Clinical implications

The immediate and long-term follow-up data of the septal reductive intervention without corrective manipulation of the mitral apparatus demonstrated good results in the haemodynamics and subjective symptoms.[22–24] However, some patients undergo recurrence of obstruction even after initial successful septal reduction. Extensive septal reduction may modify the intracavitary geometry but also increases the risk for complications. A combination of limited septal myectomy and correction of the mitral apparatus may lead to good results with a low operative risk.[24,25]

Study limitations

Overestimation of the inter-PM distance may have occurred due to arbitrarily marking the tip only in the limited number of cropped images. To reduce such overestimation, we sought to find the exact location of both PM tips by moving the axis in the volumetric images. We measured inter-PM distance and coaptation to septal distance at the mid-systolic phase (around peak T on ECG), however, due to the limited number of cropped images we could not obtain exact same time when peak pressure gradient occur. Owing to the same limitation, we could not exactly define early systole, and late systole. Therefore, regarding differences within a systolic phase, we could not find significant changes between them.

Conclusions

The current study suggests that the coaptation point, mitral tenting, PM position, and their interactions at the time when SAM is occurring, may contribute to the development of LV outflow tract obstruction. The present study found a role for geometric dynamics as one of the mechanisms of outflow obstruction. We believe our data will expand understanding of outflow tract obstruction in HCM_{SAM} and may guide the subsequent management of these patients.

Acknowledgements

We thank Yasuhiro Nakajima for his technical assistance.

Conflict of interest: none declared.

Funding

This study was partly supported by research grant of Korean Society of Echocardiography of 2009.

References

1. Autore C, Bernabo P, Barilla CS, Bruzzi P, Spirito P. The prognostic importance of left ventricular outflow obstruction in hypertrophic cardiomyopathy varies in relation to the severity of symptoms. *J Am Coll Cardiol* 2005;**45**:1076–80.
2. Maron MS, Olivotto I, Betocchi S, Casey SA, Lesser JR, Losi MA *et al.* Effect of left ventricular outflow tract obstruction on clinical outcome in hypertrophic cardiomyopathy. *N Engl J Med* 2003;**348**:295–303.
3. Henry WL, Clark CE, Griffith JM, Epstein SE. Mechanism of left ventricular outlfow obstruction in patients with obstructive asymmetric septal hypertrophy (idiopathic hypertrophic subaortic stenosis). *Am J Cardiol* 1975;**35**:337–45.
4. Klues HG, Maron BJ, Dollar AL, Roberts WC. Diversity of structural mitral valve alterations in hypertrophic cardiomyopathy. *Circulation* 1992;**85**:1651–60.
5. Klues HG, Roberts WC, Maron BJ. Morphological determinants of echocardiographic patterns of mitral valve systolic anterior motion in obstructive hypertrophic cardiomyopathy. *Circulation* 1993;**87**:1570–9.
6. Spirito P, Maron BJ, Rosing DR. Morphologic determinants of hemodynamic state after ventricular septal myotomy–myectomy in patients with obstructive hypertrophic cardiomyopathy: M mode and two-dimensional echocardiographic assessment. *Circulation* 1984;**70**:984–95.
7. Levine RA, Vlahakes GJ, Lefebvre X, Guerrero JL, Cape EG, Yoganathan AP *et al.* Papillary muscle displacement causes systolic anterior motion of the mitral valve. Experimental validation and insights into the mechanism of subaortic obstruction. *Circulation* 1995;**91**:1189–95.
8. Maron BJ, Harding AM, Spirito P, Roberts WC, Waller BF. Systolic anterior motion of the posterior mitral leaflet: a previously unrecognized cause of dynamic subaortic obstruction in patients with hypertrophic cardiomyopathy. *Circulation* 1983;**68**:282–93.
9. Shah PM, Taylor RD, Wong M. Abnormal mitral valve coaptation in hypertrophic obstructive cardiomyopathy: proposed role in systolic anterior motion of mitral valve. *Am J Cardiol* 1981;**48**:258–62.
10. Cape EG, Simons D, Jimoh A, Weyman AE, Yoganathan AP, Levine RA. Chordal geometry determines the shape and extent of systolic anterior mitral motion: in vitro studies. *J Am Coll Cardiol* 1989;**13**:1438–48.
11. Jiang L, Levine RA, King ME, Weyman AE. An integrated mechanism for systolic anterior motion of the mitral valve in hypertrophic cardiomyopathy based on echocardiographic observations. *Am Heart J* 1987;**113**:633–44.
12. Lang RM, Bierig M, Devereux RB, Flachskampf FA, Foster E, Pellikka PA *et al.* Recommendations for chamber quantification. *Eur J Echocardiogr* 2006;**7**:79–108.
13. Sasson Z, Yock PG, Hatle LK, Alderman EL, Popp RL. Doppler echocardiographic determination of the pressure gradient in hypertrophic cardiomyopathy. *J Am Coll Cardiol* 1988;**11**:752–6.
14. DeGroff CG, Shandas R, Valdes-Cruz L, Hall SA, Brickner ME, Willett DL *et al.* Utility of the proximal jet width in the assessment of regurgitant and stenotic orifices-effect of low velocity filter and comparison to actual vena contracta width: an in vitro and numerical study. *Eur J Echocardiogr.* 2000;**1**:42–54.
15. Watanabe N, Ogasawara Y, Yamaura Y, Kawamoto T, Toyota E, Akasaka T *et al.* Quantitation of mitral valve tenting in ischemic mitral regurgitation by transthoracic real-time three-dimensional echocardiography. *J Am Coll Cardiol* 2005;**45**:763–9.
16. Sherrid MV, Gunsburg DZ, Moldenhauer S, Pearle G. Systolic anterior motion begins at low left ventricular outflow tract velocity in obstructive hypertrophic cardiomyopathy. *J Am Coll Cardiol.* 2000;**36**:1344–54.
17. Henry WL, Clark CE, Roberts WC, Morrow AG, Epstein SE. Differences in distribution of myocardial abnormalities in patients with obstructive and nonobstructive asymmetric septal hypertrophy (ASH). Echocardiographic and gross anatomic findings. *Circulation* 1974;**50**:447–55.
18. Belenkie I, MacDonald RP, Smith ER. Localized septal hypertrophy: part of the spectrum of hypertrophic cardiomyopathy or an incidental echocardiographic finding? *Am Heart J* 1988;**115**:385–90.
19. Reis RL, Bolton MR, King JF, Pugh DM, Dunn MI, Mason DT. Anterion-superior displacement of papillary muscles producing obstruction and mitral regurgitation in idiopathic hypertrophic subaortic stenosis. Operative relief by posterior-superior realignment of papillary muscles following ventricular septal myectomy. *Circulation* 1974;**50**:II181–8.
20. Rodger JC. Motion of mitral apparatus in hypertrophic cardiomyopathy with obstruction. *Br Heart J* 1976;**38**:732–7.

21. Maron BJ, Nishimura RA, Danielson GK. Pitfalls in clinical recognition and a novel operative approach for hypertrophic cardiomyopathy with severe outflow obstruction due to anomalous papillary muscle. *Circulation* 1998;**98**: 2505–8.
22. ten Berg JM, Suttorp MJ, Knaepen PJ, Ernst SM, Vermeulen FE, Jaarsma W. Hypertrophic obstructive cardiomyopathy. Initial results and long-term follow-up after Morrow septal myectomy. *Circulation* 1994;**90**:1781–5.
23. Qin JX, Shiota T, Lever HM, Kapadia SR, Sitges M, Rubin DN *et al.* Outcome of patients with hypertrophic obstructive cardiomyopathy after percutaneous transluminal septal myocardial ablation and septal myectomy surgery. *J Am Coll Cardiol* 2001;**38**:1994–2000.
24. van der Lee C, ten Cate FJ, Geleijnse ML, Kofflard MJ, Pedone C, van Herwerden LA *et al.* Percutaneous versus surgical treatment for patients with hypertrophic obstructive cardiomyopathy and enlarged anterior mitral valve leaflets. *Circulation* 2005;**112**:482–8.
25. van der Lee C, Kofflard MJ, van Herwerden LA, Vletter WB, ten Cate FJ. Sustained improvement after combined anterior mitral leaflet extension and myectomy in hypertrophic obstructive cardiomyopathy. *Circulation* 2003;**108**:2088–92.